



## **Experimental Investigations on Dry Stone Masonry Walls**

G. Vasconcelos<sup>1</sup>; P. B. Lourenço<sup>1</sup>; H. Mouzakis<sup>2</sup>; L. Karapitta<sup>2</sup>

<sup>1</sup> Department of Civil Engineering, «GreetingLine» of Minho, Guimarães, Portugal.

<sup>2</sup> Department of Civil Engineering, National Technical University of Athens, Greece

### **Abstract**

Brick unreinforced masonry walls have been widely studied both from experimental and numerical point of view, but scarce experimental information is available for dry stone masonry walls that constitute the material more frequently used in the construction of ancient historical constructions. Therefore, the present work aims at increasing the insight about the behavior of typical ancient masonry walls under cyclic loading. To attain such goal, different experimental approaches are considered: static cyclic and dynamic tests. Besides the considerable out-of-plane movements of the stones, it was found that flexural response of the walls prevails in both experimental approaches.

**Keywords:** dry stone masonry walls, in-plane behavior, static cyclic tests, dynamic tests.

### **Introduction**

Although traditional masonry walls can be viewed as unsuitable structures to undergo seismic actions, they, in fact, exist and frequently represent the most important structural elements of ancient buildings. In fact, unreinforced stone masonry walls were, in the past, widely used in the construction of monumental and traditional buildings in the Northern region of Portugal. Post-earthquake research and experimental investigations revealed that if out-of-plane failure is prevented, the resistant mechanism of unreinforced masonry buildings under seismic loading is assured by in-plane behavior of masonry walls [1].

Even if northern region of Portugal has been classified as low to moderate seismicity zone, the assessment of the resisting and deformation conditions of the existing typical structural elements becomes of relevance due to the need of rehabilitation and retrofitting of ancient structures. Another reason that motivated the present research on dry stone masonry walls is related to the scarce experimental information on their in-plane behavior. In fact, most research programs in the scope of the seismic behavior focused on unreinforced brick masonry walls either from experimental or numerical points of view [2,3]. Only few experimental analyses are

available on the seismic features of stone masonry walls and particularly on dry stone masonry walls [4,5]. In the scope of seismic experimental research, distinct testing approaches have been used for unreinforced masonry structures, namely quasi-static monotonic or cyclic tests, dynamic shaking table tests and pseudo-dynamic tests. According to [6] despite dynamic tests simulate with more accuracy the seismic action, cyclic quasi-static tests enable more accurate measurements of forces and displacements and the record of damage evolution becomes easier. With respect to dynamic tests, it is more common to test complete (scaled) masonry structures, composed by masonry shear walls with or without openings, piers and diaphragms. However, few information is available on the dynamic behavior of masonry walls since important issues have to be solved in this type of tests when individual masonry walls are considered as concerns the high stiffness and the corresponding amplification of the base seismic excitation and the simulation of inertial forces by addition of external masses [7,8].

The present work aims at obtaining a better insight on the cyclic behavior of dry stone masonry walls by using both quasi-static and dynamic tests. Due to difficulties that arose in dynamic tests, different geometry was used in static and dynamic tests. This led to the impossibility of a direct comparison of the results in terms of maximum lateral resistance and even as concerns the failure modes between both experimental approaches. However, general indications about the cyclic behavior of dry stone walls may be given. In a first phase, the experimental analysis focuses on the experimental characterization of dry stone walls by static cyclic tests and in a second phase experimental results on its dynamic behavior are pointed out.

### Geometry of the walls

Dry walls can be representative of historical masonry constructions where no bonding material between stone units is present or where the major part of the bonding material with low strength properties vanished due to weathering effects. The stone used in the construction of the walls is a two mica, medium-coarsed grained granite, which is considered to be the most representative material of ancient structures existing in the Northern region of Portugal. For more details about the mechanical properties of the granite, the reader is referred to [9]. The height to length ratio was 1.2 and the wall thickness was 200mm, see Figure 1a. The height to length ratio was changed in the case of dynamic tests since a preliminary test indicated that low amplification was achieved at the top of the wall. Specimens with 750mm height, 1000mm length and 200mm thickness were adopted, see Figure 1b. Due to the connection of the wall to the bottom steel profile, a height to length ratio of 0.67 was used. The construction of dry masonry walls was quite easy and fast. After the first course, the stone units were laid in vertical position and carefully aligned during the construction.

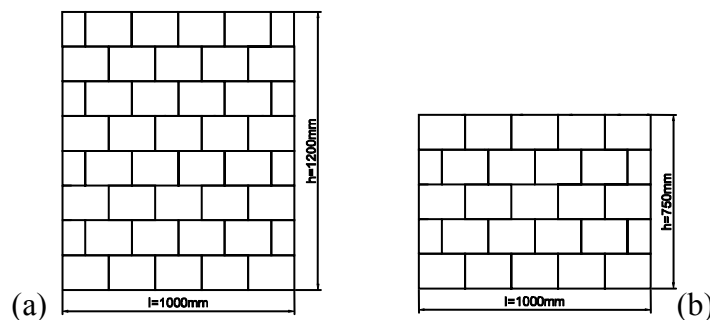


Figure 1 - Geometry of the walls, (a) Static cyclic tests, (b) Dynamic tests

## Test setup and procedure

Taking into account that masonry walls are submitted to low vertical stresses, the reference level of pre-compression adopted to simulated dead loads was 100kN, corresponding to the average normal stress  $\sigma=0.5\text{N/mm}^2$  (4 specimens). In order to evaluate the influence of the axial load on the static cyclic behavior of dry walls, two additional higher pre-compression levels were also considered: 175kN (3 specimens) and 250kN (3 specimens), corresponding to normal stresses of  $0.875\text{N/mm}^2$  and  $1.25\text{N/mm}^2$  respectively. The static cyclic tests were carried out by using the typical testing setup depicted in Figure 2a.

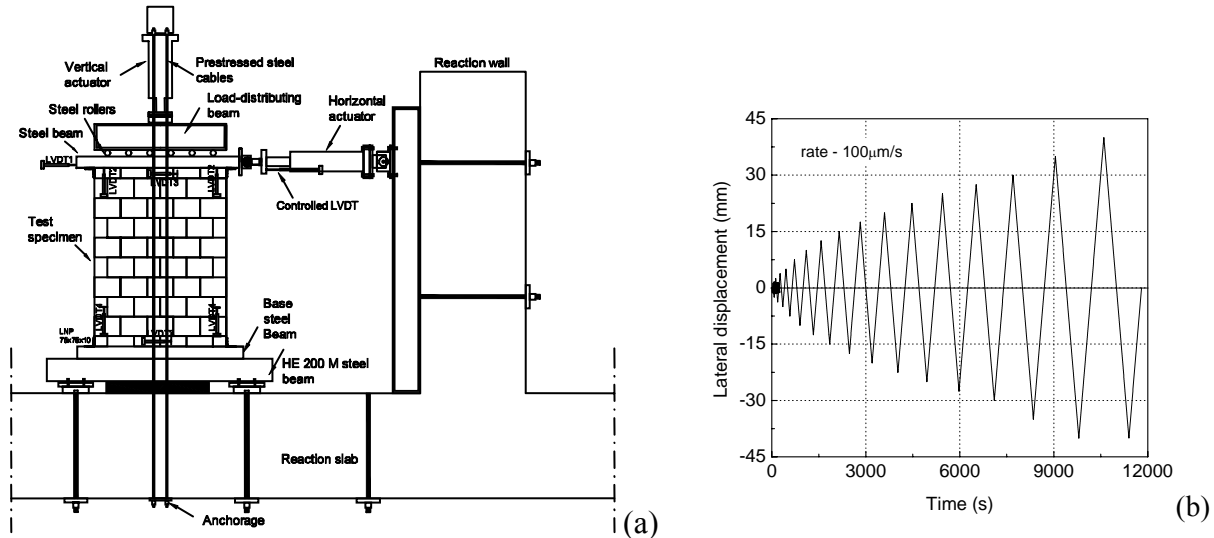
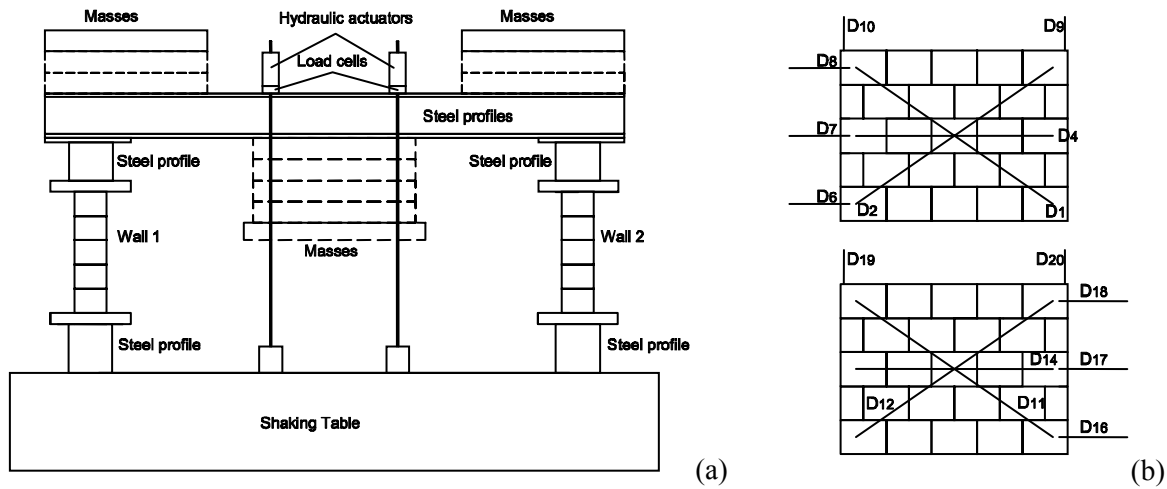


Figure 2 - Experimental details for static tests, (a) Test setup, (b) displacement-time history

The cantilever wall was fixed to the reaction slab through a couple of steel rods. The pre-compression loading was applied by means of a vertical actuator with reaction in the slab given by the cables. A stiff beam was used for the distribution of the vertical load and a set of steel rollers was added to allow relative displacement of the wall with respect to the vertical actuator. The seismic action was simulated by imposing increasing static lateral displacements according to the history indicated in Figure 2b, by means of a hinged horizontal actuator appropriately connected to the reaction wall. The deformation of the wall was measured by means of the LVDTs indicated in Figure 2a.

The dynamic tests were performed at the Laboratory for Earthquake Engineering, Athens, Greece using a steel shaking table of  $4\text{m}\times 4\text{m}\times 6\text{m}$ , with a total weight of 100kN, six independent degrees of freedom and a maximum displacement of  $\pm 100\text{mm}$ . The tests were carried out using the test setup indicated in Figure 3a. In order to save time, it was decided to test simultaneously two walls. Thus, three tests corresponding to 6 specimen walls were performed. Besides the steel profiles located at the top of each wall, six additional masses of 1Ton each were fixed on the top of the steel profile. The specimens WS1, WS2 were tested without any additional axial load. An additional vertical load of 50kN was applied in each wall in the case of walls WS3 and WS4. The load was applied by using two hydraulic actuators. In the case of tests of walls WS5 and WS6, the vertical load was replaced by 5 additional masses placed under the steel profile in order to reduce the center of mass and thus to reduce the overturning moment. The arrangement of the

steel masses adopted for these walls is indicated in the Figure 3a with dashed line. The total mass to be considered in the calculations of the inertial forces is of 3.95Ton the specimens WS1, WS2, WS3 and WS4 and of 6.55Ton in case of walls WS5 and WS6.



**Figure 3 - Experimental details for dynamic tests, (a) Test setup, (b) Location of transducers**

Instrumentation of the each specimen was organized to measure acceleration, absolute displacements and relative displacements of each wall. LVDTs D6, D7, D8 and D16, D17, D18 measure the total displacements of the walls. Diagonal cracking was measured by LVDTs D1, D2 and D11, D12, and relative displacements at the mid-height of the walls were recorded by LVDTs D4 and D14. Two additional LVDTs (D9, D10 and D19, D20) were considered to measure the possible uplift of the walls induced by flexural response, see Figure 3b. The vertical loads were measured using two load cells. In order to make the calculation of the inertial forces possible, two accelerometers were placed at the top of the steel masses. The primary test of each specimen was a uniaxial earthquake simulation using the El Centro Earthquake. For each specimen, several tests were carried out with the intensity of the reference earthquake to be increased step-wise until the collapse of each specimen. The acceleration time history of El Centro Earthquake is shown in Figure 4.

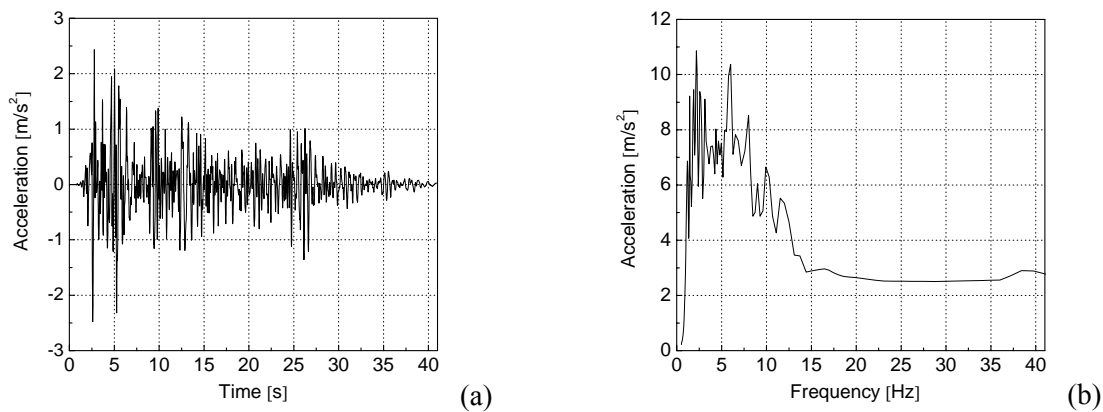


**Figure 4 - Modified (1Hz High Pass) El Centro Earthquake, (a) acceleration time history, (b) response spectrum, damping 2%**

Three tests were considered for walls WS1 and WS2 (50%, 100%, 200% El Centro Earthquake), two for walls WS3 and WS4 (200%, 300% El Centro Earthquake) and three tests were carried out in walls WS5 and WS6 (50%, 180%, 240% El Centro Earthquake).

### Results of static cyclic tests

The deformation patterns that characterize the static cyclic behavior of dry stone masonry walls were found to be quite similar for the distinct pre-compression levels, meaning that the compressive strength of the stone is too high and plays no major role in the response ( $f_c=73.0\text{N/mm}^2$ ). The behavior under cyclic reversal loading is governed by flexural response up to the maximum lateral force is reached, which is characterized by the opening of stepped cracks. The displacement at which the final stepped diagonal crack opens depends on the pre-compression level. As the lateral displacement increases and rocking mechanism develops, the effective resisting cross section to the compressive stresses is reduced and stress concentration takes place. When stress level exceeds the compressive strength of the masonry, toe crushing occurs suddenly in a brittle manner, see Figure 5a. Although this type of failure was verified for intermediate levels of pre-compression, it is particularly characteristic of dry masonry walls subjected to the highest level of pre-compression,  $\sigma=1.25\text{N/mm}^2$ . In general, toe crushing was found to occur for considerably large imposed lateral displacements.

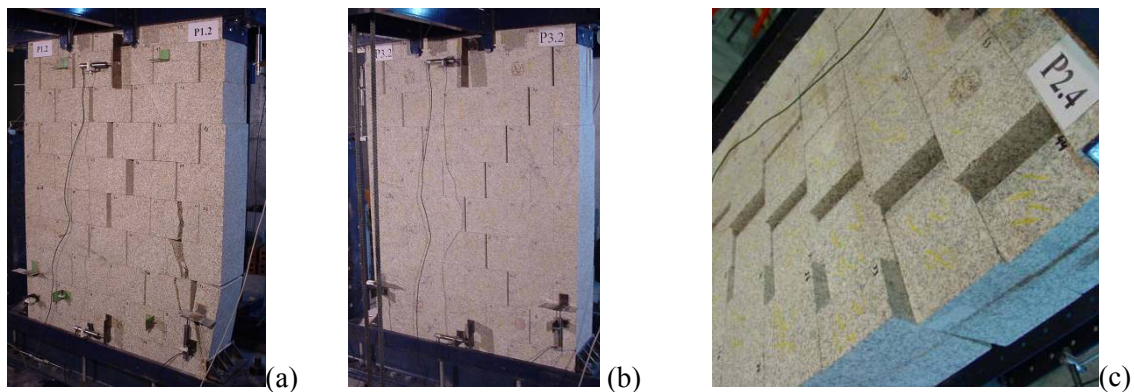


**Figure 5 - Typical failure patterns, (a) Residual displacements - wall WS1.175, (b) toe crushing and wedge formation – wall WS2.250 , (c) Out-of-plane displacements – wall WS4.100**

It should be underlined that when solely rocking mechanism is present, global collapse of the structure does not occur, see Figure 5b. However, residual inelastic horizontal displacements appeared due to sliding along bed joints of the units adjacent to the stepped flexural and diagonal cracks. Figure 5c illustrates typical out-of-plane movements of the stones recorded in dry masonry walls. The latter aspect is particularly relevant because it was insignificant in the monotonic loading tests [9]. This failure indicates that, even in the absence of out-of-plane loading, large out-of-plane movements can be found in the units adjacent to the stepped cracks due to the irregularities of the stones and to the fact they become almost loose during testing. In addition to the crack patterns and failure modes, the lateral load-lateral displacement diagrams provide valuable information on the lateral in-plane behavior. Relevant values (force, displacement) of the force-displacement diagrams, associated to particular load or damage levels, are defined. The state corresponding to the maximum lateral resistance is identified with the set

of values ( $H_{max}$ ,  $d_{max}$ ) and the first shear crack (diagonal stepped crack) is associated to the set ( $H_s$ ,  $d_s$ ). The definition of the latter values results from the visual information gathered during cyclic loading. The typical load-displacement hysteresis diagram describing the in-plane response of dry masonry walls is given in Figure 6a.

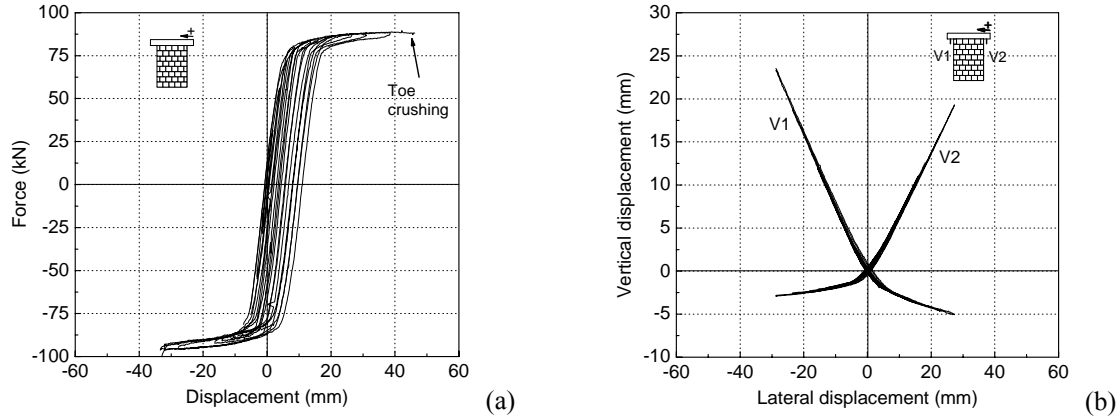


**Figure 6 - Typical diagrams for in-plane behavior, (a) Force-displacement diagram – wall WS3.175, (b) typical vertical displacement vs. lateral displacement diagrams for dry walls**

As can be observed, the shape of the typical diagram reflects, to great extent, the deformation patterns and failure modes discussed previously. In fact, the remarkable S shape of the hysteresis loops found for dry stacked masonry walls reveals the rocking mechanism that characterizes the deformation response of these walls under cyclic loading. Apart from the different maximum values of the lateral resistance and lateral displacement, all walls exhibit significant nonlinear response with almost no strength or stiffness degradation, which confirms that no damage occurs in the stone units. In spite of the large nonlinear lateral displacements, a low capacity to dissipate energy is associated to these walls. The rocking mechanism that characterizes the lateral response of dry masonry walls is also well described by the evolution of the vertical displacements with the lateral displacement of the walls as shown in Figure 6b. Note that the asymmetry of the diagram is related to the maximum close of the bed joints.

The values of maximum displacement and lateral resistance are indicated in Table 1. It is observed that some increase on the lateral strength occurs after diagonal crack opening. By comparing the results of monotonic tests obtained in [11] and the cyclic tests presented herein, one can conclude that similar values of the lateral resistance characterize the shear behavior of dry masonry walls. This is the result of the independence of dry masonry walls behavior on the displacement history for the given failure modes. Note that the values of the lateral resistance obtained for the different specimens subjected to the same axial load are rather close, which is necessarily associated to the common failure pattern. It was found that a linear correlation exist between the shear and normal stresses ( $\tau=0.382\sigma$ ,  $r^2=0.97$ ), which confirms that lateral resistance can be well described by a Coulomb type friction law. This aspect is also confirmed by the approximation of the sliding failure envelop of the composite failure criterion of Mann and Muller [2] to the experimental lateral force corresponding to the opening of the stepped diagonal crack, see also [9].

**Table 1: Relevant values of the force-displacement diagrams**

State	First diagonal crack (kN, mm)				Lateral strength (kN, mm)				
	Wall	$H_s^+$	$d_s^+$	$H_s^-$	$d_s^-$	$H_{max}^+$	$d_{max}^+$	$H_{max}^-$	$d_{max}^-$
WS1.100		32.2	6.1	-37.1	-5.1	38.8	12.8	-42.1	-18.7
WS2.100		33.4	6.4	-37.3	-5.6	37.6	9.0	-40.3	-8.3
WS3.100		33.3	5.8	-37.1	-6.0	36.5	16.3	-41.1	-19.3
WS4.100		33.1	6.2	-35.8	-4.3	35.5	24.08	-39.4	-24.8
average		33.0	6.1	-36.8	-5.2	36.9	12.8	-40.7	-17.8
WS1.175		56.4	7.2	-62.7	-7.9	61.7	20.5	-67.4	-24.4
WS2.175		57.0	7.8	-60.9	-8.0	63.2	21.7	-68.1	-23.8
WS3.175		60.0	7.4	-66.0	7.4	63.5	15.9	-67.8	-19.3
average		57.8	7.5	-63.2	7.8	62.8	22.6	-67.8	-22.5
WS1.250		81.4	9.5	-87.9	9.5	88.1	33.2	-95.3	-24.2
WS2.250		80.4	10.0	-86.9	8.9	85.1	18.4	-92.2	-16.4
WS3.250		81.2	11.8	-87.2	11.9	85.6	21.2	-91.6	-22.1
average		81.0	10.4	-87.3	10.1	86.3	24.3	-93.0	-20.9

### Results of dynamic tests

The dry stone walls were found to experience distinct failure modes associated to changes in the test setup, namely distinct axial load and the changing on the position of the steel masses. However, no significant differences were found in the natural frequency of the walls, which confirm the reliability of the test setup ( $f(WS1,2)=7.00\text{Hz}$ ,  $f(WS3,4)=7.81\text{Hz}$  and  $f(WS5,6)=7.70\text{Hz}$ ). In walls WS1 and WS2, for an intensity of 50% of the El Centro Earthquake, no relative displacements were recorded neither damage was detected, behaving both walls in the elastic regime. Even if in-plane displacements were recorded for an intensity of 100% of the El Centro Earthquake, they were almost recovered after the seismic loading was ceased. Although not very significantly, out-of-plane displacements of the walls were recorded, which are identified with the out-of-plane displacements of the stones. Significant damage and failure of the walls occurred only for an intensity of 200% of the El Centro Earthquake. The final failure patterns of walls WS2 is displayed in Figure 7a. The failure of the walls is preceded by the occurrence of rocking mechanism. After that, as the ground acceleration was increasing, diagonal stepped cracks were opening, damage of the walls grew and the collapse occurred due to toe crushing with detachment of the left side in wall WS1 and of the right side in wall WS2. This leads that large horizontal sliding displacements developed in both walls and particularly in wall WS2. It can be observed that the failure pattern is similar for both walls, which, to certain extent means that test setup is reliable and the interaction between both walls is minimal. The dynamic behavior of the walls is also well explained by the vertical displacements measured by the LVDTs located at both top upper corners. The vertical peak displacements are in accordance with the maximum accelerations of the shaking table, which means that peak accelerations lead that rocking mechanism develops. Similar behavior of both walls is also confirmed by the close values of the vertical displacements. In this case, peak displacements occur almost for the same time. The walls WS3 and WS4, to which an axial vertical load of 50kN was applied, exhibit only small residual displacements for the El Centro 200%. The dynamic response of the walls WS3 and WS4 for the El Centro 300% is governed by flexural response (rocking mechanism), with cyclic opening and closure of diagonal stepped cracks. The horizontal displacements are

practically recovered in wall WS3. Apart from the out-of-plane displacements of the stones, the final failure pattern is characterized small sidings of the stones, see Figure 7b.

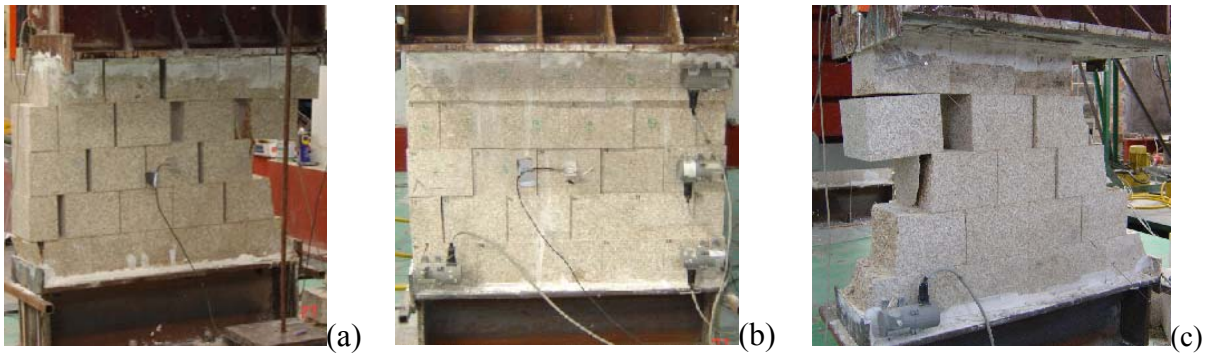


**Figure 7 - Final failure patterns, (a) Wall WS2, (b) Wall WS3, (c) Wall WS6**

Higher residual displacements are recorded in wall WS4, which is associated to horizontal sliding displacements of the stones that are visible after the seismic loading was ceased. Only thin cracks are visible in the bottom corners of the wall WS3. Similarly to what was already referred to walls WS1 and WS2, the typical rocking behavior is also confirmed by the evolution of the vertical displacements recorded for walls WS3 and WS4, see Figure 8. It is clear that the considerable positive vertical displacements measured by both vertical LVDTs reveal the tendency for the walls to rotate about the bottom corners.

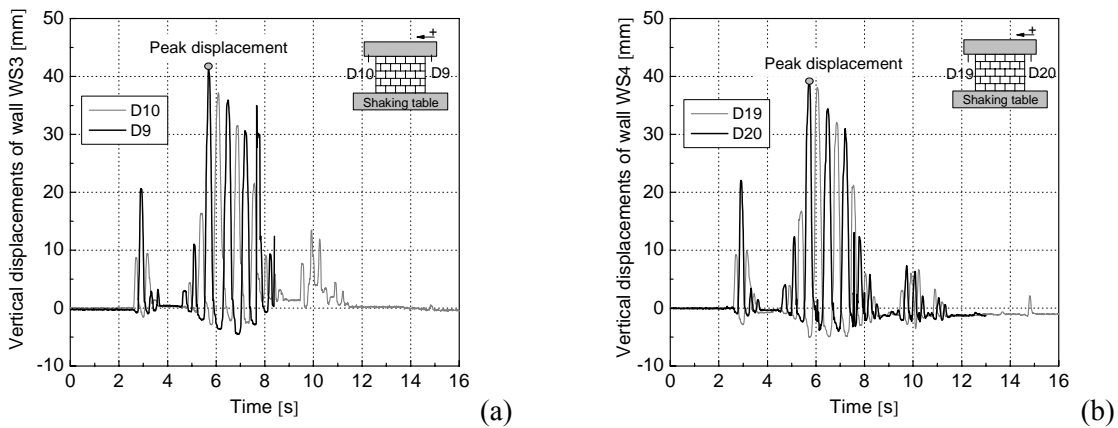


**Figure 8 - Final failure patterns, (a) Wall WS2, (b) Wall WS3, (c) Wall WS6**

No relevant events were recorded for walls WS5 and WS6 submitted to the El Centro Earthquake (50%). During the simulated El Centro Earthquake with intensity of 180%, the behavior of the walls was governed by the opening of diagonal stepped cracks with the development of horizontal sliding of the stones. This deformation pattern is clearly associated to the friction failure of the bed joints. Besides, important out-of-plane displacements developed during this seismic intensity in wall WS5. This type of displacement was not so significant in wall WS6. In both walls some damage was recorded in the stones of the bottom corners. High permanent displacement remains in wall WS5 after the test, which is directly related horizontal sliding during the seismic loading. The dynamic response of the walls for this test setup is much more characterized by a shear deformation pattern, being the vertical displacements at the top of



the wall considerably reduced (<10mm). The brittle collapse of the walls WS5 and WS6 only occurs by increasing the El Centro Earthquake to about 240%. The typical final failure mode is displayed in Figure 7c for wall WS6. It is observed that both walls fail by shear mode. In wall WS6 stepped cracks develop at the joint interface as well as through units, which means that tensile strength of the units was reached. This assumption is confirmed by the fact that stone units break into vertical pieces.

The maximum lateral forces were calculated by multiplying the maximum acceleration of the masses recorded by accelerometers and the mass of the additional steel plates and steel profiles located at the top of the walls ( $F=ma$ ). The top lateral displacement is obtained by deducting the total top displacement to the displacement measured by the LVDT placed at the bottom corner of the wall. The maximum values of the inertial forces and lateral displacements recorded in the walls for all tests are indicated in Table 2. It is observed that the response of the walls WS1 and WS2 is close in terms of inertial forces as well as in terms the maximum lateral displacements until failure occurs. Higher differences arise in the lateral displacements when failure develop, which is due to distinct horizontal sliding of the stones associated to toe crushing of the walls.

**Table 2: Relevant values for dynamic response of dry stone walls (kN, mm)**

Earthquake (%)	Wall	$H^+_{max}$	$d^+_{max}$	$H^-_{max}$	$d^-_{max}$	Wall	$H^+_{max}$	$d^+_{max}$	$H^-_{max}$	$d^-_{max}$
50		11.4	5.0	-14.3	-6.4		11.6	4.9	-12.4	-6.8
100	WS1	25.8	9.1	-20.9	5.3	WS2	24.1	7.3	-22.5	-7.2
200		46.7	35.6	-54.8	1.5		51.9	15.8	-52.1	-71.8
200	WS3	33.2	1.3	-45.0	-7.1	WS4	36.1	6.47	-42.1	-3.43
300		66.4	28.4	-60.8	-29.3		60.1	28.3	-72.9	-29.3
50		18.5	2.3	-25.3	-3.4		18.8	3.0	-18.2	-2.9
140	WS5	95.6	26.9	-90.4	-10.7	WS6	69.4	4.9	-82.2	-9.4
280		103.3	47.3	-106.3	-13.9		86.5	57.2	-109.9	-17.2

It should be noted that for the same El Centro earthquake (200%) the walls WS1 and WS2 collapsed, whereas WS3 and WS4 still exhibit considerable additional resistance. It is stressed that both walls present close values of displacement and lateral resistance, which is the result of their dynamic behaviour governed by rocking mechanism without collapse is reached. As the static cyclic tests, also the dynamic behaviour is influenced by the external vertical load applied. The values of the lateral displacement indicate the remarkable capacity of dry walls to deform without the development of significant damage if axial load is applied. The change on the test setup, by addition of steel masses under the steel profiles, leads to different failure mode. The dynamic behaviour of walls WS5 and WS6 is governed by shear failure having the rocking mechanism a minor effect on the response, which results in remarkable higher values of the inertial forces.

### Concluding remarks

In order to investigate the seismic behavior of dry stone masonry walls, a set of static cyclic tests and shaking table tests were performed. For dynamic tests, the geometry was maintained, being the vertical load and the test setup variable. For both types of test, the influence of the axial vertical load was assessed. It was possible to verify that variation on vertical load implies

variations on the failure modes of the walls as well as on the maximum lateral forces. In the static cyclic tests a Coulomb type failure criteria was found. In dynamic tests, the test setup revealed as an important factor to be taken into account in the results obtained. In fact, the reduction of the center's masse induces much more reduced overturning moments and thus of the uplift of the walls, which seems to be equivalent to the change of the boundary conditions. Although an aspect ratio of 0.67 was adopted in dynamic tests, it could be seen that rocking mechanism can even prevail in in-plane response of dry stone masonry walls. This fact can be attributed to the high strength of the stone units.

It is stressed that similar out-of-plane displacements characterize static cyclic behavior of dry stone masonry walls. This behavior is particularly relevant when stones adjacent to stair stepped cracks experiments reversed increasing displacements. This failure indicates that, even in the absence of out-of-plane solicitation, large out-of-plane movements can be found in the units adjacent to the stepped cracks due to the irregularities of the stones and to the fact they become almost loose during testing. In a real earthquake simulation, this effect can be amplified because in-plane and out-of-plane act together. Thus, the vulnerability of low interlocking stone units due to inadequate stone arrangements or inadequate shapes (e.g. round units), as well as dry or strongly deteriorated mortar joints need further studies.

## References

1. Tomažević, M., 1999, Earthquake-resistant design of masonry buildings, Imperial College Press, London. ISBN: 1-86094-066-8.
2. Mann, W., Muller, H., 1982, Failure of Shear Stressed Masonry - An Enlarged Theory, Tests and Application to Shear Walls”, The Structural Engineer, Proc. British Ceramic Society, 30, 223-235.
3. Lourenço, P.B., 1996, Computational strategies for masonry structures, PhD Thesis, Delft University of technology, Delft, The Netherlands. ISBN 90-407-1221-2. ([www.civil.uminho.pt/masonry](http://www.civil.uminho.pt/masonry))
4. Oliveira D., 2003, Experimental and Numerical Analysis of Block Masonry Structures under Cyclic Loading, PhD Thesis, University of Minho, Portugal. ([www.civil.uminho.pt/masonry](http://www.civil.uminho.pt/masonry))
5. Lourenço, P.B., Oliveira, D.V., Roca, P., Orduña, A., 2005, Dry joint stone masonry walls subjected to in-plane combined loading, Journal of Structural Engineering, ASCE, 131 (11), 1665-1673.
6. Calvi, G.M., Kingsley, G.R., Magenes, G., 1996, Testing masonry structures for seismic assessment, Earthquake Spectra, Journal of Earthquake Engineering Research Institute, 12 (1), 145-162, 1996.
7. Elgawady, M., Lestuzzi, P., Badoux, M., 2004, Dynamic versus static cyclic tests of masonry walls before and after retrofitting with FRP, Proc. 13<sup>th</sup> World Conference on Earthquake Engineering, Vancouver, Canada, paper n° 2913.
8. Moghaddam, H.A., Chinwah, J.G., Hargreaves, A.C., 1990, “Dynamic response of brick shear wall to strong ground motion”, Masonry International, 3 (3), 115-120.
9. Vasconcelos, G., 2005, Experimental investigations on the mechanics of stone masonry: characterization of granites and behavior of ancient masonry shear walls, PhD Thesis, University of Minho, Portugal. ([www.civil.uminho.pt/masonry](http://www.civil.uminho.pt/masonry))